The Journal of Headache and Pain

RESEARCH

Open Access

Nuclear paraspeckle assembly transcript 1 promotes photophobia behavior in mice via miR-196a-5p/*Trpm3* coupling

Zhuoan Huang[1,2], Xingshen Li[1], Xiaolin Wang[1], Jiaqi Wu[1], Ziyang Gong[1,2], Sulev Kõks[3*] and Minyan Wang[1,2*]

Abstract

Background The long noncoding RNA, NEAT1, is recognized as a key regulator of proinflammatory gene expression; Yet, its functional role in migraine remains unexplored, despite the central role of neuroinflammatory mechanisms in migraine pathophysiology. This study examines the implication of NEAT1 in the trigeminal ganglion activation, which underlies photophobia associated with migraine.

Methods Light aversion behavior was induced by intranasal injection of the TRPA1 activator, umbellulone. Male mouse behavior was assessed by the total time the mouse stays in the light between the dark and light compartments. To gain insight to the NEAT1-mediated photophobia mechanism, gene expression of candidate genes and non-coding RNAs interactions were assessed using RNA-sequencing, qPCR analysis, histology and dual-luciferase reporter gene assay.

Results NEAT1 was upregulated in the trigeminal ganglion of male photophobia mice; Downregulation of NEAT1 by intravenous injection of shNEAT1 adeno-associated virus vectors attenuated NEAT1 expression and alleviated photophobia-like behavior in mice. The elevated NEAT1 expression in the trigeminal ganglion of photophobia mice corresponds to the downregulation of miR-196a-5p and upregulation *Trpm3* RNA level. Predicted analysis suggested NEAT1/miR-196a-5p ceRNA network exists in photophobia mice. Indeed, knocking down NEAT1 upregulated miR-196a-5p, whilst downregulated *Trpm3* gene expression level, in the trigeminal ganglion of photophobia mice. Further investigation using dual-luciferase reporter gene assay identified NEAT1 interacting with miR-196a-5p, whilst miR-196a-5p interacting with *Trpm3*. Similar to knocking down NEAT1, TRPM3 inhibition reduced photophobia-like behavior.

Conclusion We conclude that NEAT1 is critical for promoting photophobia behavior via miR-196a-5p/*Trpm3* coupling.

Keywords NEAT1, miR-196a-5p, Transient receptor potential melastatin 3, Competing endogenous RNA, Light aversion, Migraine

*Correspondence:
Sulev Kõks
Sulev.Koks@murdoch.edu.au
Minyan Wang
Minyan.wang@xjtlu.edu.cn

[1]Department of Biosciences and Bioinformatics, School of Science, Centre for Neuroscience, Xi'an Jiaotong-Liverpool University (XJTLU), Suzhou 215123, China
[2]Institute of Systems, Molecular and Integrative Biology, University of Liverpool, Liverpool L69 7ZB, UK
[3]Personalised Medicine Centre, Perron Institute for Neurological and Translational Science, Murdoch University, Perth, WA 6009, Australia

Background

Photophobia affects up to 90% of migraineurs, with 75% continuing to face persistent sensitivity to light even during the intervals between attacks [1, 2]. The photophobia related to migraine headaches involves intricate interactions within various brain regions, including trigeminal ganglion (TG) [3, 4], and TG activation contributes to photophobia behaviour in animal models [5–7]. While previous research has predominantly focused on the contributions of neuropeptides, ion channels, cytokines and messenger RNA (mRNA) in the activation of TG [7–9], the potential roles of noncoding RNAs in photophobia have been largely overlooked. Current research on noncoding RNA associated with migraine has found that miR-155-5p in mice trigeminal nucleus caudalis [10], miR-34a-5p in rat TG cells [11] and Gm14461 lncRNA in mice TG were all important in migraine pathogenesis [12]; However, existing study on long noncoding RNAs (lncRNAs) in migraine is lacking.

Nuclear paraspeckle assembly transcript 1 (NEAT1) is a ubiquitous nuclear-retained lncRNA and expressed in a variety of mammalian cell types{Bond, 2009 #1085}. NEAT1 plays significant roles in cellular pathophysiology and is among the most extensively researched lncRNAs [13]. NEAT1 stands out for its substantial impact on neurodegenerative diseases [14]. NEAT1 is also heavily implicated in the function of the immune system and in inflammatory response in neuropathic pain [15] by increasing proinflammatory genes in the dorsal root ganglion of rats [14] and enhancing the expression of cytokines via competing endogenous RNA (ceRNA) mechanism [16]. While NEAT1 is well-established as a regulator of inflammatory gene expression in the pain disorder and neuroinflammatory mechanisms are central for migraine pathophysiology, its direct mechanistic link to migraine, especially its role in driving trigeminovascular sensitisation and migraine progression, remains unexplored.

The intricate relationships between noncoding and coding RNAs, especially through the ceRNA mechanism, present a novel perspective for understanding the molecular underpinnings of migraine [17]. There are several studies on ceRNA networks in neuropathic pain and neuroinflammation [18, 19], while existing studies on ceRNA in migraine are limited with only one focusing on ceRNA networks of circRNA-miRNA-mRNA in the plasma of migraine patients [20]. There are no reports of ceRNA networks in the nervous system of preclinical animal models of migraine.

To bridge these gaps in knowledge, this study investigated the role of NEAT1 in photophobia using the recently established rapid-onset mouse photophobia model [9] and explored how NEAT1 might exert its regulatory mechanism involving the ceRNA network. We first investigated how lncRNAs and miRNAs alter in the TG of photophobia mice; Then explored the role of NEAT1 in light aversion behavior and its regulatory mechanism via NEAT1/miR-196a-5p and miR-196a-5p/*Trpm3* coupling. The data unravelled a novel photophobia-specific mechanism by which NEAT1 promotes photophobia behavior via NEAT1/miR-196a-5p/*Trpm3* axis.

Methods

Animal preparation

A total of 115 adult male C57BL/6J mice (21.13 ± 0.16 g, mean ± SEM), aged at 6–7 weeks were purchased from Shanghai SLAC Laboratory Animal Corporation Ltd. China. All mice were sourced from four cohorts and housed in groups of 3–5, unless otherwise stated, on a 12 h light cycle with food and water *ad libitum*. All behavior experiments were housed in the Experimental Animal Centre of Soochow University for at least one week and acclimated to the housing room before use. Animals from each cohort were randomly allocated to different experimental groups with the same experimental procedure in order to reduce bias and minimise potential confounders, particularly considering mice were sourced from different cohorts and the potential influence of mice remembering the light/dark configuration on light aversion behavior under bright light [21]. For all experiments, animal size was decided based on earlier publication in the field [7, 9]. Investigators handled animals with extra care to reduce any distress and blinded. Animal procedures were approved by the Ethical Review Panels of Xi'an Jiaotong-Liverpool University under the agreement with Soochow University and performed in accordance with relevant China national and provincial guidelines.

Photophobia behavior assay and experimental design

The rapid-onset photophobia model was induced by intranasal injection (*i.n.*) of a selective transient receptor potential ankyrin 1 (TRPA1) agonist, 1 μmol/kg umbellulone (UMB, SML0782 Sigma-Aldrich) and mouse behavior was observed in a customized black & white box using a light source (J&K Photoelectronic) and video tracking system (Hikvision) as we recently reported [9]. Briefly, on day 1, each mouse underwent two acclimation sessions in the testing chamber under dim light for 35 min, separated by a 15-minute recovery period in their home cage. On day 2, mice were acclimated once using the same protocol as day 1, followed by a 35-minute recording under bright light to establish self-control conditions. After rapid photophobia induction and a 15-minute recovery period, mouse behavior was recorded for 35 min. Two behavior study series were designed in this study.

In series 1, we designed a shNEAT1-AAV (adeno-associated virus) vector to knock down NEAT1 (Genechem,

China) and its negative control (NC) to explore the role of NEAT1 in photophobia mice. These AAVs (2.50E + 13v.g./kg shNEAT1-AAV or 2.50E + 13v.g./kg AAV-NC) or vehicle (phosphate buffer saline, PBS, 09-8912-100, Medicago, Sweden) were systemically injected via tail vein 14 days before the start of mice acclimation sessions (Supplemental Fig. 1). After behavior recording, the TG tissue was immediately dissected, snap-frozen in liquid nitrogen and stored in -80 degree for measuring expression levels of NEAT1 and its potential target miRNAs and mRNAs.

In series 2, we explored the role of NEAT1-targeted mRNA-encoding protein, TRPM3, in photophobia mice. The experimental groups included: (i) The TRPM3 selective antagonist, isosakuranetin (ISO, 10 mg/kg, BaoJi Herbest Bio-Tech Co., Ltd, China) in photophobia mice *(i.n.* 150 μg/kg UMB); (ii) Vehicle *(i.p.* 0.25% DMSO) group in photophobia mice (*i.n.* 150 μg/kg UMB) only; (iii) Control group (*i.p.* 0.25% DMSO) in mice without photophobia (*i.n.* 0.2% DMSO). Either ISO or its vehicle was intraperitoneally injected (*i.p.*) for two consecutive days (Supplemental Fig. 2). The test drug was injected between the two acclimations on day 1, followed by another injection on day 2 immediately after the photophobia induction.

Mouse behavior was analysed by categorizing responders to UMB/vehicle administration. Responders were defined as those mice whose total time in the light box (total time in light) fell outside mean ± 1 SD (excluding mice treated with either shNEAT1-AAV in Series 1 or ISO treatment in Series 2). Only responders were included for further experiments and statistical analysis. The total time in light was quantified as a behavioral parameter to assess the degree of light avoidance. Given that photophobia involves motor activity, transition times between the light and dark boxes was also assessed.

Adeno-associated viral vector production

In order to knock down NEAT1 in mice, we used the adeno-associated virus (AAV) vector serotype 9 that express short hairpin RNA (shRNA) targeting the sequence of NEAT1 (GCTTCCAAAGCGCCTTTA ACA) or negative control (TTCTCCGAACGTGTCA CGT). These AAVs were synthesised and cloned into GV478 (U6-MCS-CAG-EGFP) vector with *BsmB*I sites (Shanghai Genechem Co., Ltd.). The recombinant vector was detected by DNA sequencing. The viral vector was transfected into 293T cells using lipofectamine 2000 (Invitrogen; Thermo Fisher Scientific, Inc.) together with plasmids pHelper and pRepCap. AAV were harvested 72 h post-transfection and AAV9 were purified through iodixanol gradient ultracentrifuge and subsequent concentration. Purified AAV viruses were titrated using a qPCR-based method. All the AAV produced were administered to mice in the photophobia behavior assay in series 1.

Histological examination

Histological examination was conducted in order to validate the AAV infection efficiency of shNEAT1-AAV/AAVNC-infected cells of the mouse TG. Mice injected with shNEAT1-AAV, AAVNC or PBS were anesthetised by 5% isoflurane and transcardially perfused with PBS, followed by 4% paraformaldehyde (P804537, Macklin, Shanghai, China). The TG from either side were collected, and fixed using 4% paraformaldehyde at 4 °C overnight. The tissues were dehydrated in 10%, 20%, and 30% sucrose (V900116, Sigma-Aldrich, St. Louis, MO, USA) solutions at 4 °C overnight, then embedded in Tissue-Tek O.C.T. Compound (4583, Sakura, Flemingweg, Netherlands). TG Sect. (20 μm) were prepared using a cryostat (CM1950, Leica, Tokyo, Japan), fixed on glass slides and incubated in 4′,6-diamidino-2-phenylindole (DAPI, C1005, Beyotime, Shanghai, China) for 5 min. The intensity of the enhanced green fluorescent protein (EGFP) was imaged using a confocal laser scanning microscope (LSM880, Zeiss, Jena, Germany) after addition of the mounting solution (P0126, Beyotime, Shanghai, China).

RNA sequencing

RNA sequencing was used to investigate how lncRNAs and miRNAs alter in the TG of photophobia mice. To minimise the animal use, we promptly dissected TG from the photophobia mice induced by UMB *(i.n.* 150 μg/kg) and control mice (*i.n.* 0.2% DMSO) following behavior recording, as reported earlier [9]. The combined left and right TG of each mouse were rapidly homogenated in liquid nitrogen, aliquoted and stored at -80 degree (906GP-ULTS, Thermo Scientific, Finland) for total RNAs extraction. One aliquot RNA samples were shipped to Beijing Genomics Institute (BGI, Shenzhen, China) for cDNA library construction using MGIEasy RNA Library Prep Kit (1000005276, MGI, Shenzhen, China) for lncRNAs and MGIEasy Small RNA Library Prep Kit (BGI-Shenzhen, China) for miRNAs. The library was amplified using Phi29 DNA polymerase (A39392, Thermo Fisher Scientific, Waltham, MA, USA) to generate DNA nanoballs (DNBs) containing more than 300 copies. Finally, the DNBs were sequenced using combinational probe anchor synthesis-based DNBSEQ-500 sequencer (BGI, Shenzhen, China) for lncRNAs and using G400 platform (BGI-Shenzhen, China) to generate sequencing reads of SE50 bases length for miRNAs.

Screening altered LncRNAs, miRNAs and mRNAs

Following RNA-sequencing, we identified candidate lncRNAs and miRNAs in the TG of photophobia mice by comparing them to the control. Mouse reference genome

version GRCm39 was used for whole genome transcriptome analysis, and Salmon was used to call quantified transcripts of individual samples [22]. For differential analysis of the transcript expressions, DEseq2 package and its functions were used. Comparisons between photophobia vs. control were performed and FDR correction was applied for nominal *P*-values. In order to make comparisons among different groups, genes with multiple Ensembl Gene IDs were consolidated. Differential lncRNAs and miRNAs were determined as those with an adjust *P*-value < 0.05 and| log2foldchange| > 0. Differential expressed mRNAs were screened using the same protocol, the results of which have been reported in our previous study [9].

Quantitative polymerase chain reaction (qPCR)

Quantitative PCR analysis was used to validate RNA-seq data using. We used the TG tissues and RNA from the same animal cohort as those for RNA-sequencing. The total RNAs were reverse transcribed to cDNA using GoScript Reverse Transcription System (A5001, Promega) for NEAT1 and mRNAs. For miR-196a-5p, cDNA was synthesised using the stem-loop method using miRNA 1st Strand cDNA Synthesis Kit (MR101, Vazyme). Peptidylprolyl isomerase A (PPIA), β-actin (ACTB), U6 and 18 S were used as reference genes. Primers for NEAT1 and mRNAs were designed using Primer Premier 5 and primers for miR-196a-5p, U6 and 18 S were designed using miRNA Primer Design or provided by Vazyme (Table 1). All primers were validated prior to qPCR analysis. The qPCR reaction was performed using GoTaq qPCR Master Mix (A6002, Promega) and miRNA Universal SYBR qPCR Master Mix (MQ101, Vazyme) in QuantStudio 5 Real-Time PCR System (Applied Biosystems). The level of individual RNA was normalised to the geometric mean of β -actin and PPIA or 18 S and U6 using the $2^{-(\Delta Ct)}$ method.

Table 1 The forward and reverse primer sequences of selected RNAs for qPCR analysis

Gene	Accession	Primer sequences (5′ – 3′)	
Neat1	NR_131212.1	Forward	AGGAGAAGCGGGGCTAAGTA
		Reverse	TAGGACACTGCCCCCATGTA
Trpm3	XM_036161558.1	Forward	TATGTACCATAGGTATCGCCC
		Reverse	GGTATGGTCGGACTACATCTC
Slc7a2	NM_007514.3	Forward	GGGGTCATTTCTGCTGTGA
		Reverse	GCTGGTCATAACACAAGCCA
Rnf38	NM_175201.7	Forward	TAGCAACCACCAGTCAGAGC
		Reverse	GGCAGGTACGGTTTCCCTTA
miR-196a-5p	MIMAT0000518	Forward	CGCGCGTAGGTAGTTTCATGTT
		Reverse	AGTGCAGGGTCCGAGGTATT
ACTB	NM_007393.5	Forward	CTGTCCACCTTCCAGCAGAT
		Reverse	CGCAGCTCAGTAACAGTCCG
PPIA	NM_017101.1	Forward	TTGCTGCAGACATGGTCAAC
		Reverse	TGTCTGCAAACAGCTCGAAG
U6	19,862	Forward	CTCGCTTCGGCAGCACA
		Reverse	AACGCTTCACGAATTTGCGT
18 S	19,791	Forward	GTTCCGACCATAAACGATGCC
		Reverse	TGGTGGTGCCCTTCCGTCAAT

Prediction of miRNA-mRNA/lncRNA coupling and ceRNA network construction

In order to predict the potential interactions between altered miRNA-mRNA and altered miRNA-lncRNA, we used the widely cited, recently updated miRNA targeting databases based on CLIP-seq, various high-throughput sequencing data and experimentally verified miRNA-target interactions. Starbase and miRWalk were simultaneously used to predict putative miRNA–mRNA interactions, and only mRNAs that were jointly predicted by both databases were included in this study [23, 24]. For lncRNAs, those predicted by the starBase and TargetScan databases were all included in this study [24, 25]. Additionally, miRTarBase serves as a comprehensive repository of miRNA-target interactions that have been experimentally validated by reporter assays, Western blot analysis, microarray and next-generation sequencing [26]. Subsequently, we augmented the results obtained from the aforementioned screening process by incorporating the miRNA-target interactions documented in miRTarBase.

Based on the above miRNA-mRNA/lncRNA interactions, we applied those mRNAs and lncRNAs that were both altered following photophobia induction for constructing miRNA-lncRNA/mRNA interactions. According to ceRNA theory, lncRNAs or mRNAs have inverse relationships with miRNAs; mRNAs and lncRNAs have positive associations. Thus, two regulatory scenarios will be taken into account: (i) up-regulated lncRNA-downregulated miRNA-upregulated mRNA; (ii) downregulated lncRNA-upregulated miRNA-downregulated mRNA. So, the Pearson correlation coefficient for lncRNAs and mRNAs that were targeted by the same miRNA were calculated, and the mRNA- lncRNA pairs with $r > 0$, $p < 0.05$ were chosen. The ceRNA network was visualised with Cytoscape software [27].

Dual-luciferase reporter gene assay

In order to further determine the interaction between NEAT1 and Mir196a-1/2, *Trpm3* and Mir196a-1/2, a dual-luciferase reporter gene assay was performed using a detection kit according to the manufacturer's protocol (Promega, Wisconsin, USA). The reporter constructs containing the lncRNA NEAT1 wild-type (WT) or mutant (Mut) 3′-UTR were transfected into human embryonic kidney (HEK) 293-T cells with miR-196a-5p

mimic or mimic NC using lipofectamine 3000 reagent (miR-196a-5p is the mature sequence of Mir196a-1/2). After a 48-hour transfection, the relative luciferase activity of the cells was tested using the Dual-Luciferase Assay System (Promega). Similarly, the targeting binding relationship between *Trpm3* and miR-196a-5p was determined using the methods mentioned above. Each transfection was performed six times.

Data presentation and statistical analysis

Raw experimental data were analysed using GraphPad Prism 9.4.1. Normality test was performed for all quantitative data by Shapiro-Wilk test. For comparisons between two independent groups, if the data passed the normality test, the data were presented as mean ± SEM and analysed by one-way ANOVA was used for comparison of independent groups, followed by unpaired t-test; if not, the data were analysed by Kruskal–Wallis followed by Mann-Whitney test. The criteria used for data exclusion during the analysis is that, for a normally distributed data set, the outlier points were removed by eliminating any points that were beyond (mean ± 3* standard deviation); For an abnormally distributed data set, the outlier points were removed by eliminating any points that were beyond (Q3 + 1.5*IQR) (Q1: first quartile, Q3: third quartile, IQR: interquartile range). For data between two dependent experimental groups (before and after pretreatment of test drugs), paired t-test was used for comparison. Data presentation of each quantitative data set was described in respective figure legend. Significant differences were shown by $P < 0.05$, $P < 0.01$, $P < 0.001$, or $P < 0.0001$.

Results

Induction of NEAT1 gene expression in the TG of photophobia mice

RNA-sequencing analysis showed a profound alteration of lncRNAs in the TG of photophobia mice when compared with control group. Among a total of 125 lncRNAs altered (Fig. 1A), 106 (84.8%) lncRNAs were upregulated while 19 (15.2%) downregulated (Fig. 1B). Particularly noted was that the upregulation of NEAT1 by photophobia (*padj* = 0.0151, $n = 7$, Fig. 1C). Further qPCR analysis showed a consistent increase in the RNA level of NEAT1 ($P = 0.0489$, $n = 7$, Fig. 1D) with the quantitative difference attributable to methodological variations between RNA-seq and qPCR detection. These findings indicate a rapid activation of TG, associated with differentially expressed lncRNAs, especially NEAT1, following photophobia induction.

Knockdown NEAT1 alleviated light aversion behavior in mice

Given the notable upregulation of NEAT1 following photophobia testing (Fig. 1), we explored the role of NEAT1 in mice exhibiting photophobia. shNEAT1-AAV9 vector was administered to mice intravenously to achieve global NEAT1 knock down. AAV-NC and the vehicle (PBS) was injected as controls. After a 14-day incubation period, light aversion was induced, followed by the behavior assessment. We found that intranasal injection of UMB (150 μg/kg, *i.n*) to mice markedly reduced total time in light in the PBS control group (147.8 ± 58.96s, $P = 0.0005$, $n = 11$, Fig. 2A) when compared to its self-control (427.1 ± 58.93s), indicating successful induction of light aversion behavior. Similar light avoidance was also observed in mice administered with AAV-NC (2.50E + 13v.g./kg, *i.v.*, 156.5 ± 41.42s, $n = 11$) when compared to the self-control (326.7 ± 34.63s, $P = 0.0005$, $n = 11$, Fig. 2. C), suggesting the AAV negative control does not affect light aversion behavior. Differently, such light avoidance was not observed in NEAT1 knock down mice by shNEAT1-AAV (2.50E + 13v.g./kg, *i.v.*, 730.4 ± 187.5s, $n = 12$) when compared to its self-control (621.8 ± 149.2s, $P = 0.1083$, $n = 12$, Fig. 2B), suggesting knocking down NEAT1 counteracted the light avoidance. Further analysis showed that the total time in light after injection of shNEAT1-AAV (468.7 ± 76.23s, $n = 10$) was significantly higher than that in PBS (98.10 ± 35.04s, $P = 0.0002$, $n = 10$) or AAV-NC group (126.2 ± 31.27s, $P = 0.0007$, $n = 10$, Fig. 2D). Consistently, when the data were presented as relative values, normalised to self-control, to minimise variations and animal memory effects in the bright light, mice administered with shNEAT1-AAV had significantly higher total time in light (1.013 ± 0.1281, $n = 11$) compared to that in the vehicle group (0.1617 ± 0.04581, $P < 0.0001$, $n = 11$) or the AAV negative control group (0.4592 ± 0.09446, $P = 0.0012$, $n = 11$, Fig. 2E). Additionally, mice with NEAT1 knocking down via shNEAT1-AAV exhibited no significant difference in baseline transition times compared to negative controls prior to photophobia induction. However, following photophobia induction, shNEAT1-AAV-treated mice showed markedly increased transition times relative to shNEAT1-AAV-NC control (Supplementary Fig. 3). Collectively, the above data demonstrated that knocking down NEAT1 can alleviate mouse light aversion behavior and the associated motor activity.

To confirm the effectiveness of NEAT1 knockdown, we examined the RNA level of NEAT1 in TG cells of all mice infected with AAV that targets the EGFP sequence in the AAV vector, using histological examination. The results showed that TG cells in mice injected with shNEAT1-AAV or AAV negative control, but not PBS, had successful AAV infection as shown in cyan (Fig. 2F),

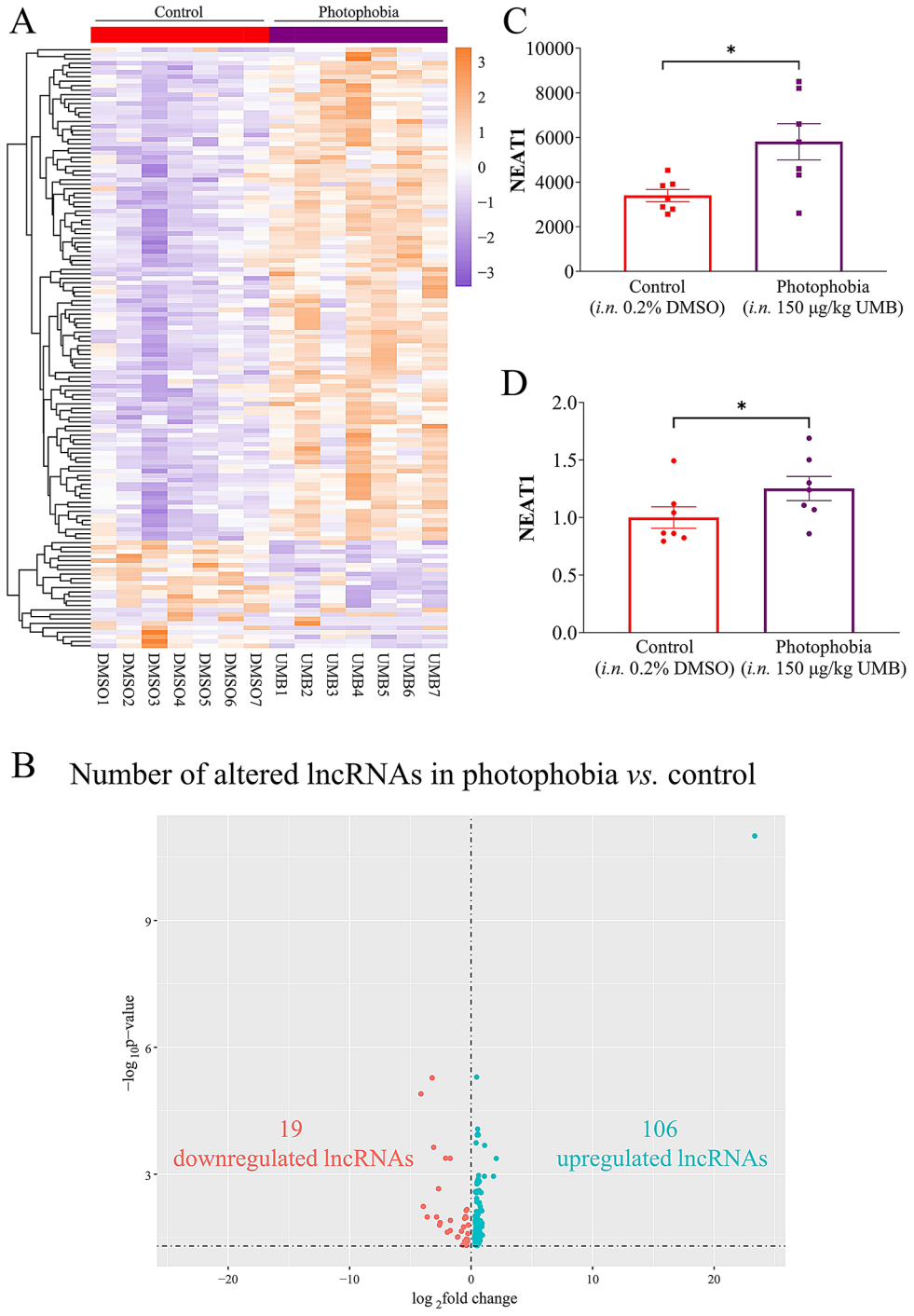

Fig. 1 RNA-sequencing analysis of TG revealed profound alternation of RNA levels of lncRNAs in the light aversion behavior mice. (**A**) The heatmap showed the levels of 125 altered lncRNAs in each sample of control (vehicle) and photophobia (UMB) group respectively. (**B**) The volcano plot depicted the numbers of downregulated and upregulated lncRNAs (|log2FoldChange|≥0, adjusted P-value ≤ 0.05) following photophobia. Each dot represents an RNA, and red and blue dots indicate down- and up-regulation, respectively. (**C**) Analysis of RNA-sequencing data to compare RNA levels of NEAT1 in the TG tissue of mice between the photophobia group and control group. (**D**) qPCR validation of NEAT1 RNA level in the TG of mice in photophobia group and control group, presented by the fold changes normalized to the geometric mean of the two reference genes (β-actin and PPIA). One-tailed unpaired t-test was used for comparisons among two independent groups. Significant differences were indicated by ns not significant, * $P < 0.05$

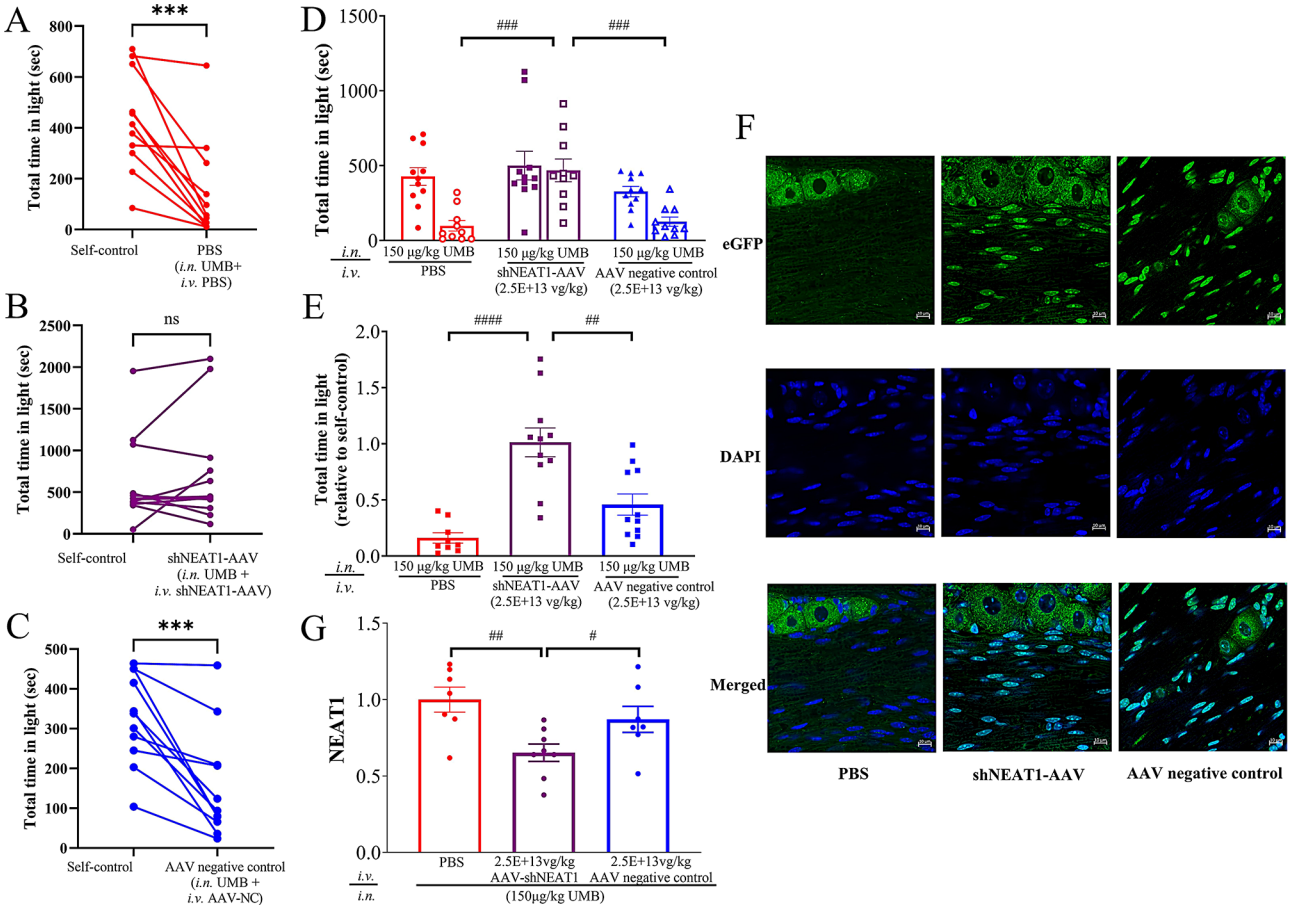

Fig. 2 Knockdown of NEAT1 alleviated C57BL/6J mouse light aversion behavior induced by intranasal injection of UMB. Light aversion was induced by intranasal injection (*i.n.*) of UMB (150 μg/kg). There was a total of three experimental groups: (1) photophobia (PBS, vehicle, *i.v.*), NEAT1 knockdown (2.5E + 13vg/kg AAV-shNEAT1, AAV, *i.v.*) and AAV negative control (2.5E + 13vg/kg AAV-NC, AAVNC, *i.v.*) groups. AAV-shNEAT1, AAV-NC and PBS were tail-vein injected 14 days prior to photophobia induction. Light aversion behaviour of each mouse was recorded before and after light aversion induction for self-comparison. (**A**-**C**) Total time in light (sec) of individual mouse before and after light aversion induction in the PBS (**A**), shNEAT1-AAV (**B**) and AAV-NC (**C**) groups. (**D**) Comparisons of total time in light (sec) after light aversion induction between the PBS and AAV, shNEAT1-AAV and AAV-NC groups. (**E**) Comparison of total time in light normalised to respective self-control among the PBS, shNEAT1-AAV, AAV and AAV-NC groups. (**F**) Representative images showing histological examination of AAV-infected cells in the TG of photophobia mice compared with the PBS control. (**G**) qPCR data on RNA levels of NEAT1 in the TG of three groups presented by the fold changes normalized to the geometric mean of the two reference genes (β-actin and PPIA). Blue indicates TG cell nucleus stained by DAPI; Green indicates cells infected by AAV vector. Group data were presented as mean ± SEM. One-tailed unpaired t-test was used for comparisons among two independent groups. Significant differences were indicated by ns not significant, * $P < 0.05$, ** $P < 0.01$, *** $P < 0.001$, or **** $P < 0.0001$; $^{\#}P < 0.05$, $^{\#\#}P < 0.01$, $^{\#\#\#}P < 0.001$. *Indicates comparison between dependent groups. $^{\#}$Indicates comparison between independent groups

indicating successful AAV infection within the TG. Additionally, quantitative analysis demonstrated that NEAT1 was downregulated in the TG of shNEAT1-AAV mice (0.6527 ± 0.05710, $n = 8$) compared to the PBS group (1.000 ± 0.08208, $P = 0.0018$, $n = 8$) and AAV-NC group (0.8711 ± 0.2254, $P = 0.0242$, $n = 8$, Fig. 2G). This data underscores the efficacy of the knockdown approach for investigating the behavior outcomes of NEAT1 depletion. Taken all together, these data confirmed that NEAT1 knockdown effectively alleviated mouse light aversion behavior, suggesting the importance of NEAT1 in light aversion involving TG activation.

Prediction of an upregulated ceRNA network modulated by NEAT1 in the TG of light aversion mice

Given the critical role of NEAT1 in light aversion, we explored how NEAT1 could potentially regulate photophobia by influencing the ceRNA network in the TG. miRNA sequencing and qPCR analysis identified a total of 7 differentially expressed miRNAs in mice exhibiting photophobia compared to the control (Fig. 3A), of which Mir-133a-2, Mir-33 and Mir-3106 were upregulated, and Mir-196a-1, Mir-196a-2, Mir-767 and Mir-5119 downregulated (Fig. 3B). Based on the ceRNA theory [17], lncRNAs can act as competing molecules by binding to miRNAs, thereby regulating the expression of mRNA.

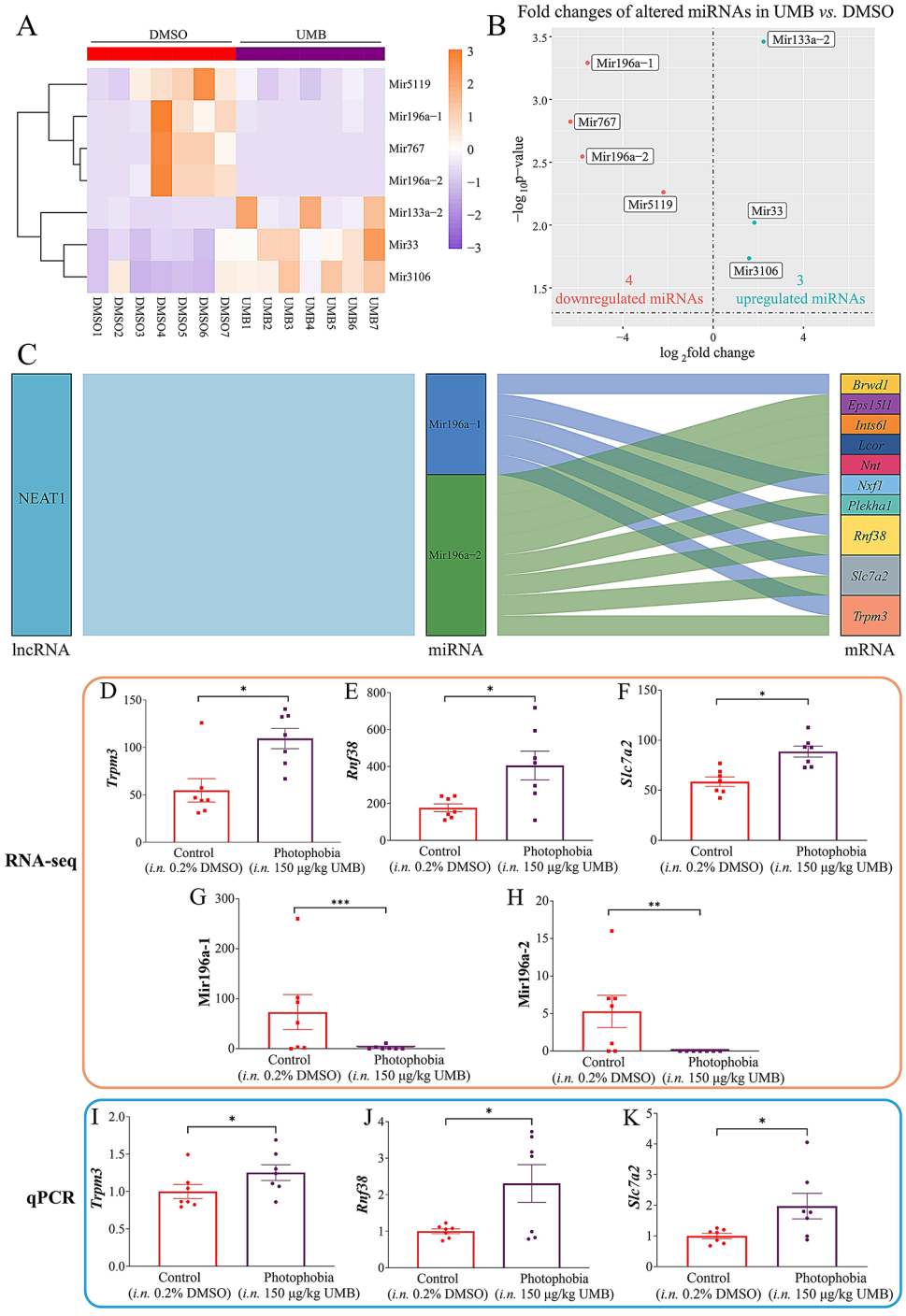

Fig. 3 An upregulation ceRNA network modulated by NEAT1 was predicted in the TG of light aversion mice. (**A**) The heatmap showed the RNA level of 7 altered miRNAs in each sample of control (DMSO) and photophobia (UMB) groups. (**B**) The volcano plot depicted the numbers of 7 differentially expressed lncRNAs (|log2FoldChange|≥0, adjusted P-value ≤ 0.05) between UMB vs. DMSO groups, of which 4 downregulated, while 3 upregulated. (**C**) A Sankey Diagram illustrated the interactions of the RNAs among the upregulatory ceRNA network modulated by NEAT1 in the TG of light aversion mice. The expression level of *Trpm3* (**D**), *Rnf38* (**E**), *Slc7a2* (**F**), Mir196a-1 (**G**) and Mir196a-2 (**H**) in TG of control and photophobia mice accessed by RNA sequencing analysis. Validation of the gene expression of *Trpm3* (**I**), *Rnf38* (**J**) and *Slc7a2* (**K**) in the TG of mice in photophobia group and control group using qPCR. Group data were presented as mean ± SEM. One-tailed unpaired t-test was used for comparisons among two independent groups. Significant differences were indicated by ns not significant, * $P < 0.05$, ** $P < 0.01$, *** $P < 0.001$, or **** $P < 0.0001$

Therefore, we integrated sequencing data from miRNAs, along with differentially expressed mRNAs and lncRNAs induced by photophobia, and utilised four online databases containing mRNA-miRNA and lncRNA-miRNA interactions to construct a ceRNA network. We identified lncRNA-miRNA-mRNA interactions from the databases based on a positive correlation in expression trends between lncRNAs and mRNAs, as well as a negative correlation in the expression trends between miRNA and lncRNA/mRNAs, as derived from the RNA sequencing data. The results revealed the prediction of an upregulated ceRNA network in the TG of photophobia mice, which include NEAT1, Mir-196a-1, Mir-196a-2 and 10 mRNAs (Fig. 3C).

Within this network, Mir-196a-1 and Mir-196a-2 were the only miRNAs identified, both of which serve as pre-miRNAs for miR-196a-5p. This made miR-196a-5p a compelling candidate for further investigation. Therefore, we focused on miR-196a-5p for further validation to refine and narrow down the list of potential targets. In consistent with the RNA-sequencing results (Fig. 3D-F), the qPCR analysis confirmed that 3 differentially expressed genes, *Trpm3*, *Rnf38* and *Slc7a2*, were all upregulated by photophobia (Fig. 3I-K). Due to the limited quantity of TG tissue available, which was insufficient for further qPCR analysis, RNA levels of the miRNAs were exclusively represented by RNA-sequencing data, showing downregulation of Mir-196a-1 and Mir-196a-2 when compared to the control (Fig. 3G and H). These findings demonstrated the upregulated ceRNA network involves NEAT1, miR-196a-5p, and the three targeted mRNAs, indicating a potential pathway through which NEAT1 in the TG contributes to photophobia behavior.

NEAT1 enhances miR-196a-5p/Trpm3 axis following photophobia behavior

Among the three novel mRNAs identified, *Trpm3* was identified to have a strong target potential as it was targeted by both Mir-196a-1 and Mir-196a-2 within the upregulated ceRNA network; while other mRNAs were targeted by only one miRNA. Additionally, *Trpm3*-encoding protein, TRPM3, has been previously reported to function in meningeal terminals of the TG nerve [28]. We therefore validated the predicted ceRNA network by assessing the RNA level of *Trpm3* and miR-196a-5p in the TG of all photophobia mice injected with PBS, shNEAT1-AAV and AAV-NC groups. The results revealed that miR-196a-5p was upregulated in the NEAT1 knockdown group (1.230 ± 0.3486, $n = 8$) compared with the PBS control group (0.4431 ± 0.1501, $P = 0.0296$, $n = 6$), showing a similar increasing trend to the AAV-NC group, although it did not reach statistical significance (1.230 ± 0.3486, $n = 8$, Fig. 4A). On contrary, *Trpm3* was downregulated in the NEAT1 knockdown group (0.6146 ± 0.05270, $n = 8$) compared to the PBS control (1.000 ± 0.1375, $P = 0.0158$, $n = 7$) and negative AAV control (1.007 ± 0.1524, $P = 0.0193$, $n = 8$, Fig. 4B). These findings suggest that that knocking down NEAT1 leads to the upregulation of miR-196a-5p and downregulation of *Trpm3*, in the TG of photophobia mice, aligning with the predictions of the ceRNA theory.

Sequence-based binding site predictions indicate that miR-195a-5p has potential binding sites with both NEAT1 (Fig. 4C) and *Trpm3* (Fig. 4D), but not their mutations. It is worth noting that the miR-196a-5p–binding site at the *Trpm3* 3′-UTR and NEAT1 is evolutionarily conserved among human and mouse (Fig. 4E & F), suggesting that regulation of TRPM3 by miR-196a-5p and NEAT1 is functionally important. We therefore investigated whether NEAT1 could potentially influence photophobia through its physical interactions with miR-196a-5p and the interaction between miR-196a-5p and *Trpm3*, using dual-luciferase reporter gene assay. The results revealed that miR-195a-5p mimic (0.6855 ± 0.005067, $n = 6$), but not its negative control (1.00 ± 0.02104, $P < 0.0001$, $n = 6$, Fig. 4G), was able to robustly reduce the luciferase activity driven by the 3′-UTR of NEAT1 in HEK 293-T cells. Such reduction vanished when a mutation was introduced to the predicted seed sequence of NEAT1 3′-UTR ($P = 0.8821$, $n = 6$, Fig. 4G). The interaction between miR-196a-5p and *Trpm3* yielded similar results, demonstrating that, compared to its negative mimic (1.00 ± 0.01712, $n = 6$), the miR-196a-5p mimic reduced the luciferase activity driven by the 3′-UTR of *Trpm3* (0.9062 ± 0.01039, $P < 0.0001$, $n = 6$), indicating its inhibitory effect on *Trpm3* expression (Fig. 4H). Such reduction was not observed when a mutation was introduced to the predicted seed sequence of *Trpm3* 3′-UTR ($n = 6$, Fig. 4H). These findings confirmed the coupling of miR-196a-5p/NEAT1 and miR-196a-5p/*Trpm3* in HEK 293-T cells. Taken together, our data revealed that NEAT1 promotes photophobia behavior via miR-196a-5p/*Trpm3* axis.

TRPM3 inhibition by isosakuranetin reduced light aversion behavior in mice

We further confirmed the role of TRPM3 in light aversion by intraperitoneally administrating the TRPM3 selective antagonist, ISO (10 mg/kg) or its vehicle (0.25% DMSO) to mice for two consecutive days prior to inducing photophobia behavior. As we reported earlier [9], the results showed a successful induction of photophobia behavior after intranasal injection of UMB when compared to the control group (Fig. 5). The total time in light (129.7 ± 32.97s, $n = 10$) was significantly lower after photophobia induction than that in control (266.5 ± 68.29s, $P = 0.0461$, $n = 10$, Fig. 5D). Similar to knocking down

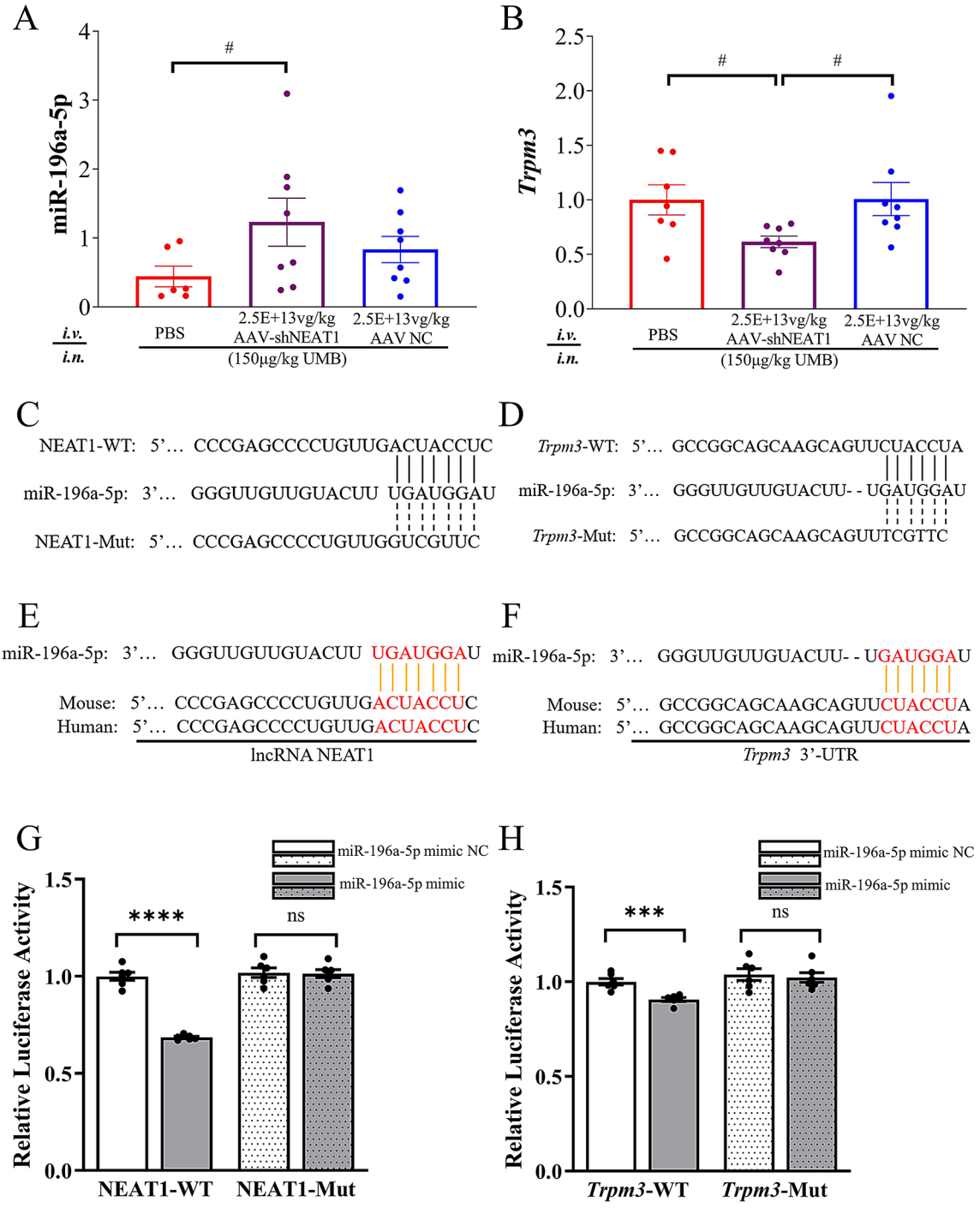

Fig. 4 NEAT1 knockdown upregulated miR-196a-5p while downregulated *Trpm3* following photophobia induction via miR-196a-5p/*Trpm3* axis. Effects of NEAT1 knockdown on RNA levels of miR-196a-5p (**A**) and *Trpm3* (**B**) in the TG of mice in the PBS, shNEAT1-AAV and AAV-NC groups following light aversion induction. In A and B, RNA levels were normalized to the geometric mean of β-actin and PPIA (*Trpm3*), U6 and 18 S (*miR-196a-5p*) and were represented. (**C**) Predicted miR-196a-5p binding sites in the region of NEAT1. (**D**) Predicted miR-196a-5p binding sites in the region of *Trpm3*. (**E**) RNA sequences of NEAT1 in human and mouse, which are highly conserved and possess a conserved miR-196a-5p–binding region. (**F**) RNA sequences of the 3′-UTRs of *Trpm3* in human and mouse, which are highly conserved and possess a conserved miR-196a-5p–binding region. (**G**) Dual-luciferase reporter assay verifying the interaction between the 3′-UTR of NEAT1 and miR-196a-5p. Data are representative of 6 independent experiments. (**H**) Dual-luciferase reporter assay verifying the interaction between the 3′-UTR of *Trpm3* and miR-196a-5p. Data are representative of 6 independent experiments. The fold changes in qPCR were normalized to the geometric mean of β-actin and PPIA(*Trpm3*), U6 and 18 S(*miR-196a-5p*) and RNA levels were determined using $2^{-\Delta CT}$ method. NC, negative control; WT, wild-type; Mut, mutant. Group data were presented as mean ± SEM. One-tailed unpaired t-test was used for comparisons among two independent groups. Significant differences were indicated by ns not significant, * $P < 0.05$, ** $P < 0.01$, *** $P < 0.001$, or **** $P < 0.0001$; $^{\#}P < 0.05$, $^{\#\#}P < 0.01$, $^{\#\#\#}P < 0.001$. *Indicates comparison between dependent groups. $^{\#}$Indicates comparison between independent groups

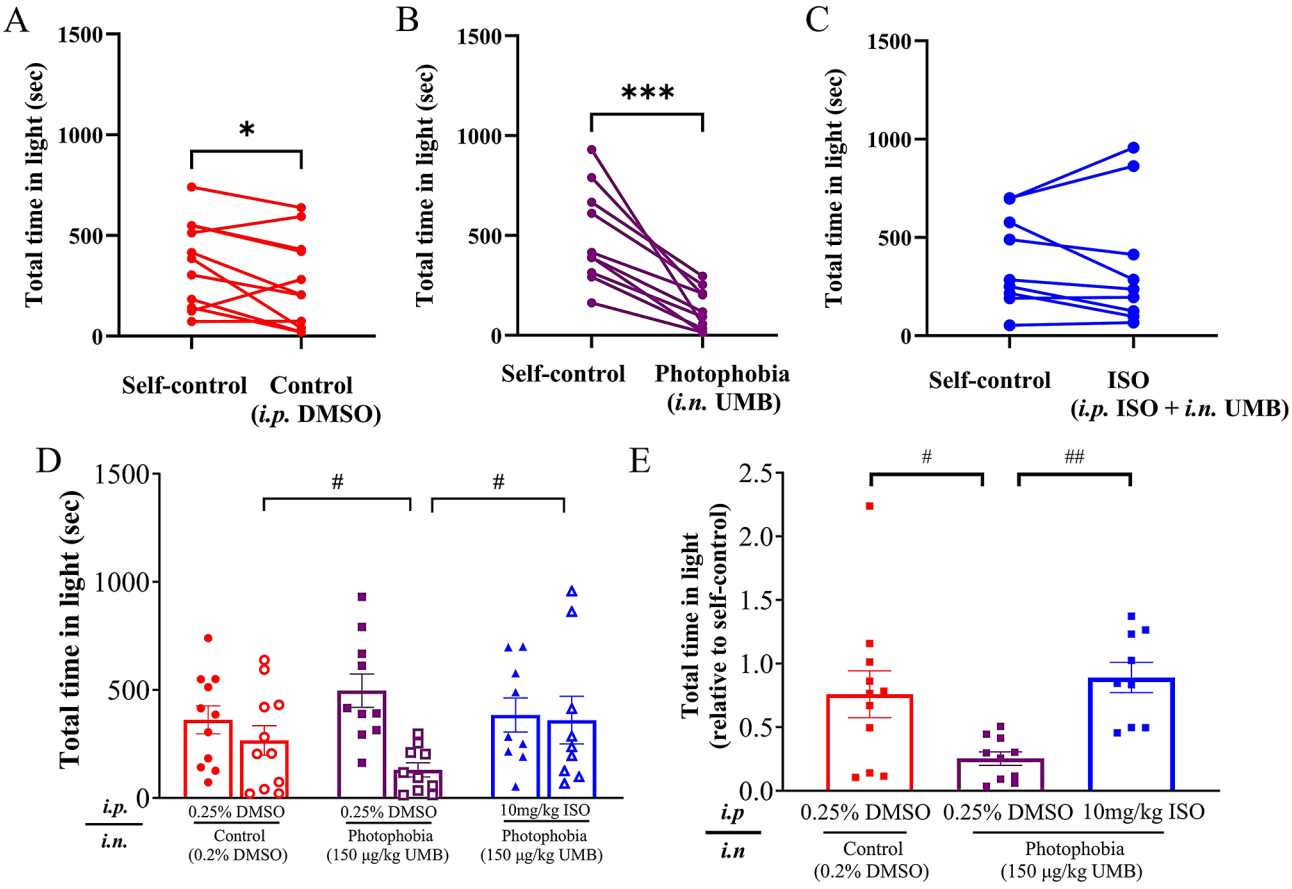

Fig. 5 Inhibition of TRPM3 reversed the photophobia behavior of C57BL/6J induced by intranasal injection of UMB. Light aversion was induced by intranasal injection (*i.n.*) of UMB (150 μg/kg). 0.2% DMSO was injected as the model control. There was a total of three experimental groups: control group (vehicle control, *i.p.* 0.25% DMSO.), photophobia group in the absence (*i.p.*, 0.25% DMSO*)* or presence of the TRPM3 inhibitor, ISO (*i.p.*,10 mg/kg). ISO or its vehicle was intraperitoneally injected for 2 consecutive days prior to photophobia induction. (**A**-**C**) Comparison of total time in light (sec) before and after light aversion induction in the control (**A**), photophobia (**B**) and photophobia + ISO (**C**) groups. (**D**) Effects of ISO on light avoidance before and after light aversion induction by comparing total time in light (sec) between the control and photophobia, or photophobia and ISO groups. (**E**) Effects of ISO on total time in light (normalised to self-control) following light aversion induction. Group data were presented as mean ± SEM. One-tailed, unpaired t-test was used for comparisons between two independent groups. Significant differences were indicated by ns not significant, * $P < 0.05$, ** $P < 0.01$, *** $P < 0.001$, or **** $P < 0.0001$; $^{\#}P < 0.05$, $^{\#\#}P < 0.01$. *Indicates comparison between dependent groups. $^{\#}$Indicates comparison between independent groups

NEAT1, such photophobia behavior was reversed by pre-treatment of ISO as the total time that photophobia mice spent in the light zone restored to a similar level as the control (360.2 ± 109.9s, $P = 0.007$, $n = 9$, Fig. 5D). Consistently, when the data were presented as relative values, normalised to self-control, to minimise animal memory effects in the bright light, photophobia mice had a significantly lower total time in light (0.2532 ± 0.05387, $n = 9$) than the model control (0.7592 ± 0.1840, $P = 0.0110$, $n = 11$, Fig. 5E). Such reduction was counteracted by the pretreatment with ISO (0.8916 ± 0.1186, $P = 0.0326$, $n = 9$, Fig. 5E). It was noted that a slight, yet statistically significant decrease in the total time in light was observed in the model control group compared to its self-control ($P = 0.0213$, $n = 11$, Fig. 5A), potentially attributable to the effect of the vehicle used. Additionally, analysis also revealed that the photophobia mice exhibited reduced baseline transition times compared to the model control. Differently, pretreatment of ISO restored the transition times following photophobia induction (Supplementary Fig. 4). Collectively, these findings revealed that, similar to NEAT1 knock down, TRPM3 inhibition reduces mouse light aversion behavior.

Discussion

NEAT1 is a stress-responsive transcript at cellular level and is crucial for fine-tuning brain functions to enable adaptive behaviour in response to various stress [29]. Our study reveals that NEAT1 plays a pivotal role in photophobia mechanism through the activation of ceNRA network within the trigeminal ganglion. The present findings demonstrate: (i) trigeminal ganglion activation in photophobia mice involving profound lncRNA alterations including the upregulation of NEAT1; (ii) reduction of

NEAT1 expression in the TG and alleviated light aversion behavior when NEAT1 is knocked down; (iii) elevation of NEAT1 expression corresponds to downregulation of miR-196a-5p and upregulation *Trpm3* RNA level in the TG of photophobia mice; (vi) predicted NEAT1/miR-196a-5p ceRNA network in photophobia mice; (v) upregulation of miR-196a-5p and downregulated *Trpm3* gene expression level, in the TG of photophobia mice when NEAT1 is silenced; (vi) NEAT1 interacting with miR-196a-5p, whilst miR-196a-5p interacting with *Trpm3* at cellular level; (vii) alleviated photophobia-like behavior by TRPM3 inhibition. Collectively, these observations support the crucial role of NEAT1 in photophobia mechanism by which NEAT1 within the TG contributes to photophobia via NEAT1/miR-196a-5p/*Trpm3* axis. Lastly, the data highlight a potential novel therapy for migraine prevention with activity against NEAT1/miR-196a-5p/*Trpm3* pathway.

NEAT1 is ubiquitously expressed in the central nervous system, with high expression in glial cells and low expression in neurons [29]. Building on the existing data, we first confirmed NEAT1 expression in the mouse TG, the tissue essential for processing signals associated with photophobia behaviour [5–7, 9]. This data suggest NEAT1 is implicated in the TG function. Our results then reveal a rapid upregulation of NEAT1 expression in the TG following light aversion induced by an activator of a stress-sensing cation channel, TRPA1, while silencing NEAT1 by shNEAT1-AAV vectors correspondingly alleviates light aversion behavior. These findings highlight the significance of NEAT1 as a key regulatory lncRNA in photophobia pathogenesis. Whereases this is, to our knowledge, the first study pointing a lncRNA functions in migraine-related mechanism, earlier studies have already investigated alterations of NEAT1 in stressed cells [30], as well as in models of anxiety [29], neurodegenerative diseases [14] and neuropathic pain [15]. For instance, in line with our findings, global NEAT1 knockout ($Neat1^{-/-}$ mice) displays a distinct behavioural phenotype manifested in decreased anxiety [29]. Consistently, in neuropathic pain models, NEAT1 increases proinflammatory genes by stabilising its interacting mRNAs in the dorsal root ganglion of rats [14], and overexpression of NEAT1 enhances the expression of cytokines [16]. Therefore, we propose that NEAT1 plays a pivotal role in stress signaling, including photophobia induction, and altered NEAT1 expression is a common feature in multiple neurological disorders [14–16], which may underlie certain common phenotypes including behaviour and neuroinflammation. Further, the profound lncRNA alterations and the prompt NEAT1 upregulation in the TG following light aversion induction suggests NEAT1-mediated TG activation in processing photophobia. Given that light aversion is induced by UMB that can trigger headache via activating TRPA1 to transmit stress signal to the trigeminovascular system, our data offer new insights into the functional interplay between NEAT1 and TG activation in photophobia mechanism.

How does NEAT1 contribute to photophobia? According to the proposed ceRNA theory in 2011 [17], lncRNA-miRNA-mRNA interactions may the mechanism underlying this observation. Previous research has revealed ceRNA interactions play a role in the development of neurological and cancer conditions. For instance, NEAT1 regulates spinal cord injury-induced neuropathic pain via miR-128-3p/AQP4 axis in rats [16] and NEAT1 promotes colorectal cancer cell proliferation and migration via coupling miR-196a-5p in human colon cancer cell lines [31]. In the current study, we report that, in the TG, downregulation of Mir-196a-1 and Mir-196a-2, the two pre-miRNAs for miR-196a-5p, corresponds to the upregulation of NEAT1 following photophobia. Additionally, the miR-196a-5p was upregulated in the TG of photophobia mice when NEAT1 is knocked down. These data imply a close association of NEAT1 with miRNA-196a-5p following photophobia. Further data by dual-luciferase reporter gene assay showed a physical interaction between miR-196a-5p and NEAT1 in HEK293 T cells, supporting their coupling following photophobia. These findings approve the importance of NEAT1 in contributing photophobia involving miR-196a-5p and extend previous report on the role of miR-196a-5p in Huntington's disease and spinal and bulbar muscular atrophy models [32–34].

What might be the specific target RNA that compete with NEAT1 for miR-196a-5p? We previously reported an upregulation of *Trpm3* gene expression in the TG of photophobia mice [9]. In this study, such alteration following photophobia is restored when NEAT1 is silenced, which corresponds to the reduction of miR-196a-5p; Similar as NEAT1, *Trpm3* also bind to miR-196a-5p in HEK293 T cells. Based on these data, we propose *Trpm3* as the target mRNA that can compete with NEAT1 for miR-196a-5p during photophobia processing. This data has clinical implications as the organisation of the *Trpm3* genes is highly conserved in mice, rats and humans, indicating common functions of their gene products [35]. Furthermore, our bioinformatic analysis predicts a NEAT1/miR-196a-5p/*Trpm3* network in photophobia mice. Taken together, these findings represent a previously unrecognised mechanism underlying the NEAT1-regulated photophobia by which NEAT1 competes with *Trpm3* by coupling with miRNA-196a-5p as a ceRNA network.

The organisation of the *Trpm3* genes is highly conserved in mice, rats and humans, indicating common functions of their gene products [35]. The importance of *Trpm3* axis in photophobia is confirmed by examining

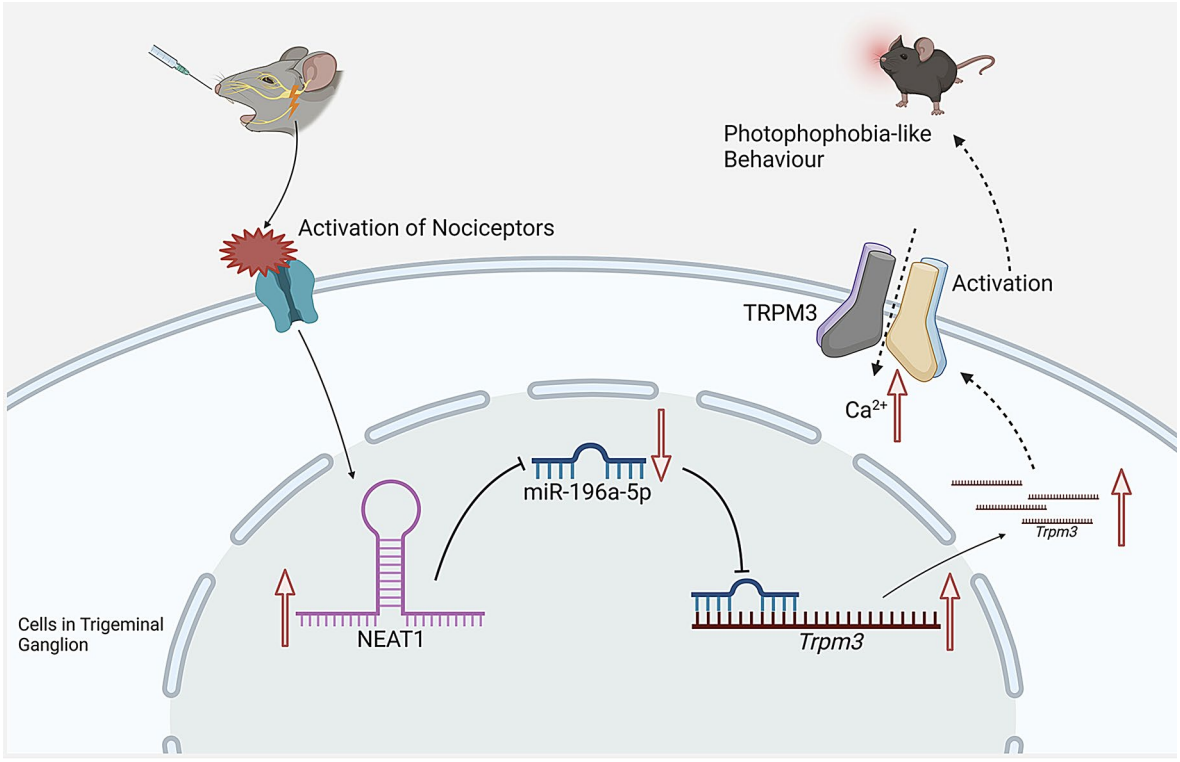

Fig. 6 Schematic representation of the proposed regulatory mechanism of NEAT1 in UMB-induced light aversion via miR-196a-5p/*Trpm3* axis. Triggers of photophobia, such as UMB, upregulate gene expression of NEAT1, which enhances *Trpm3* gene expression by inhibiting miR-196a-5p expression and activity through competing endogenous RNA mechanism. This upregulation of *Trpm3* gene expression may lead to the production of the TRPM3 protein, whose activation sustains trigeminovascular sensitization via calcium influx and neuroinflammation, ultimately affecting photophobia behavior. The figure was created in BioRender. Lab, M. (2025). https://BioRender.com/bem83j5. TRPA1, Transient receptor potential ankyrin type 1. TRPM3: Transient receptor potential melastatin-3

the role of the *Trpm3*-encoding protein, TRPM3. TRPM3 is a multimodal calcium-permeable cation channel with a specific expression pattern, including cells in the brain, eye, kidney, sensory neurons of the peripheral system [36, 37]. TRPM3 channel can profoundly activate peripheral trigeminal nerve fibers in mouse meninges with its selective agonists in mice [38]. In line with these findings, in this study, inhibition of TRPM3 ameliorates mouse light aversion behavior, supporting that TRPM3 plays a crucial role of in maintaining trigeminal ganglion sensitisation in driving photophobia processing and supporting the NEAT1/miR-196a-5p/*Trpm3* ceRNA network involvement in photophobia.

Our study has limitations. First, we identified NEAT1 upregulation corresponds to miR-196a-5p downregulation in the photophobia model and their physical interactions in HEK293 T cells, but lack of direct measurement of their interaction in the photophobia model, which prevents us from conclusively state the role of NEAT1/miR-196a-5p/*Trpm3* axis in photophobia. Second, we identified gene expression of *Trpm3* in the TG, but TRPM3 production and its activity were not assessed in the model when NEAT1 is knockdown. Third, migraine predominantly affects females [2], and nociceptive firing induced by a TRPM3 activator is particularly prominent for female mice [38]; However, the role of NEAT1 and TRPM3 were not assessed in female mice in the present study. Further investigation into future comparative gender analysis is warranted. Therefore, caution should be noted when extrapolating these findings to human conditions. Considering the NEAT1 expression in the TG and its functional significance in photophobia, future studies should investigate cell-type-specific NEAT1 distribution patterns and NEAT1/miR-196a-5p interaction within TRPM3-positive TG neurons and satellite glial cells. Additionally, investigation of NEAT1's role in complementary behavior assessment (e.g., head-scratching, Von Frey filament assays and facial allodynia evaluation) would provide valuable insights into various migraine-related phenotypes. While NEAT1 is well-established as a regulator of inflammatory gene expression in the pain disorder [16] and neuroinflammatory mechanisms are central for photophobia and migraine pathophysiology, a direct mechanistic link between NEAT1 and neuroinflammation in driving trigeminovascular sensitisation or headache progression also worth future exploration.

Conclusion

This study reveals a crucial role of NEAT1 in contributing to photophobia processing in mice involving NEAT1/miR-196a-5p/*Trpm3* ceRNA network activation. We propose a novel regulatory mechanism of photophobia by which migraine triggers, such as UMB, stimulate nociceptors of trigeminal ganglion, inducing NEAT1 and *Trpm3* expression, which compete for binding to miR-196a-5p in driving trigeminal ganglion sensitisation, leading to photophobia. The induction of *Trpm3* gene expression may lead to the production of TRPM3, playing a role in maintaining trigeminovascular sensitisation through calcium influx and neuroinflammation, ultimately influencing photophobia behavior (Fig. 6). This finding provides novel insights into the molecular mechanisms underpinning photophobia and suggests NEAT1 as a potential therapeutic target for photophobia.

Abbreviations

TG	Trigeminal ganglion
lncRNAs	Long noncoding RNAs
NEAT1	Nuclear paraspeckle assembly transcript 1
mRNA	Messenger RNA
ceRNA	Competing endogenous RNA
i.n.	Intranasal injection
NC	Negative control
i.p.	Intraperitoneally injected
AAV	Adeno-associated virus
shRNA	Short hairpin RNA
EGFP	Enhanced green fluorescent protein
DNBs	DNA nanoballs
qPCR	Quantitative polymerase chain reaction
PPIA	Peptidylprolyl isomerase A
ACTB	β-actin
WT	Wild-type
Mut	Mutant
HEK	Human embryonic kidney
UMB	Umbellulone
ISO	Isosakuranetin
DMSO	Dimethyl sulfoxide
TRPA1	Transient receptor potential ankyrin 1
TRPM3	Transient receptor potential melastatin 3

Supplementary Information

The online version contains supplementary material available at https://doi.org/10.1186/s10194-025-02057-5.

Supplementary Material 1

Acknowledgements

We thank Lingdi Nie for helpful discussions and Shiyan Wang for technical support.

Author contributions

ZH, XL, XW and ZG performed the experiments and analyzed the data. ZH prepared all the figures and drafted the manuscript. MW and ZH designed the experiments. MW and SK supervised ZH, edited the manuscript. MW designed, sponsored, drafted, and edited the manuscript. All authors have reviewed the manuscript.

Funding

This work was supported by Wangwenli Charitable Foundation, China (RSD0006) and XJTLU research fund.

Data availability

No datasets were generated or analysed during the current study.

Declarations

Ethics approval and consent to participate

Animal procedures were approved by the Ethical Review Panels of Xi'an Jiaotong–Liverpool University under the agreement with Soochow University and performed in accordance with relevant China national and provincial guidelines. Ethical approval code: ER-SRR-10886166202311271327 32.

Consent for publication

Not applicable.

Competing interests

The authors declare no competing interests.

Received: 18 March 2025 / Accepted: 30 April 2025
Published online: 22 May 2025

References

1. Oakley CB, Kossoff EH (2014) Migraine and epilepsy in the pediatric population. Curr Pain Headache Rep 18:402. https://doi.org/10.1007/s11916-013-0402-3
2. Migraine (2017) Annals of Internal Medicine 166, ITC49-ITC64 https://doi.org/10.7326/AITC201704040
3. Noseda R, Copenhagen D, Burstein R (2019) Current Understanding of photophobia, visual networks and headaches. Cephalalgia 39:1623–1634. https://doi.org/10.1177/0333102418784750
4. Wang Y, Wang S, Qiu T, Xiao Z (2022) Photophobia in headache disorders: characteristics and potential mechanisms. J Neurol 269:4055–4067. https://doi.org/10.1007/s00415-022-11080-4
5. Mason BN, Kaiser EA et al (2017) Induction of Migraine-Like photophobic behavior in mice by both peripheral and central CGRP mechanisms. J Neurosci 37:204–216. https://doi.org/10.1523/jneurosci.2967-16.2016
6. Recober A, Kuburas A et al (2009) Role of calcitonin Gene-Related peptide in Light-Aversive behavior: implications for migraine. J Neurosci 29:8798–8804. https://doi.org/10.1523/jneurosci.1727-09.2009
7. Kuburas A, Mason BN et al (2021) PACAP induces light aversion in mice by an inheritable mechanism independent of CGRP. J Neurosci 41:4697–4715. https://doi.org/10.1523/JNEUROSCI.2200-20.2021
8. Takacs-Lovasz K, Kun J et al (2022) PACAP-38 induces transcriptomic changes in rat trigeminal ganglion cells related to neuroinflammation and altered mitochondrial function presumably via PAC1/VPAC2 Receptor-Independent mechanism. Int J Mol Sci 23. https://doi.org/10.3390/ijms23042120
9. Huang Z, Yao J et al (2024) Gender-different effect of Src family kinases antagonism on photophobia and trigeminal ganglion activity. J Headache Pain 25:175. https://doi.org/10.1186/s10194-024-01875-3
10. Manack A, Buse DC, Serrano D, Turkel CC, Lipton RB (2011) Rates, predictors, and consequences of remission from chronic migraine to episodic migraine. Neurology 76:711–718. https://doi.org/10.1212/WNL.0b013e31820d8af2
11. Hautakangas H, Winsvold BS et al (2022) Genome-wide analysis of 102,084 migraine cases identifies 123 risk loci and subtype-specific risk alleles. Nat Genet 54:152–160. https://doi.org/10.1038/s41588-021-00990-0
12. Xu M, Yan Y et al (2020) Effects of long non-coding RNA Gm14461 on pain transmission in trigeminal neuralgia. J Inflamm 17:1. https://doi.org/10.1186/s12950-019-0231-1
13. Dong P, Xiong Y et al (2018) Long Non-coding RNA NEAT1: A novel target for diagnosis and therapy in human tumors. Front Genet 9. https://doi.org/10.3389/fgene.2018.00471
14. Li K, Wang Z (2023) LncRNA NEAT1: key player in neurodegenerative diseases. Ageing Res Rev 86:101878. https://doi.org/10.1016/j.arr.2023.101878
15. Maruyama M, Sakai A et al (2023) Neat1 LncRNA organizes the inflammatory gene expressions in the dorsal root ganglion in neuropathic pain caused by nerve injury. Front Immunol 14. https://doi.org/10.3389/fimmu.2023.1185322
16. Xian S, Ding R, Li M, Chen F (2021) LncRNA NEAT1/miR-128-3p/AQP4 axis regulating spinal cord injury-induced neuropathic pain progression. J Neuroimmunol 351:577457. https://doi.org/10.1016/j.jneuroim.2020.577457

17. Salmena L, Poliseno L, Tay Y, Kats L, Pandolfi PP (2011) A CeRNA hypothesis: the Rosetta stone of a hidden RNA Language? Cell 146:353–358. https://doi.org/10.1016/j.cell.2011.07.014
18. Morchio M, Sher E, Collier DA, Lambert DW, Boissonade FM (2023) The role of MiRNAs in neuropathic pain. Biomedicines 11:775
19. Zeng M, Zhang T, Lin Y, Lin Y, Wu Z (2023) The common LncRNAs of Neuroinflammation-Related diseases. Mol Pharmacol 103:113–131. https://doi.org/10.1124/molpharm.122.000530
20. Lin J, Shi S, Chen Q, Pan Y (2020) Differential expression and bioinformatic analysis of the circrna expression in migraine patients. Biomed Res Int 2020(4710780). https://doi.org/10.1155/2020/4710780
21. Kaiser EA, Kuburas A, Recober A, Russo AF (2012) Modulation of CGRP-induced light aversion in wild-type mice by a 5-HT(1B/D) agonist. J Neurosci 32:15439–15449. https://doi.org/10.1523/JNEUROSCI.3265-12.2012
22. Patro R, Duggal G, Love MI, Irizarry RA, Kingsford C (2017) Salmon provides fast and bias-aware quantification of transcript expression. Nat Methods 14:417–419. https://doi.org/10.1038/nmeth.4197
23. Campbell M, Sticht C, De La Torre C, Parveen A, Gretz N, miRWalk (2018) An online resource for prediction of MicroRNA binding sites. PLoS ONE 13. https://doi.org/10.1371/journal.pone.0206239
24. Li JH, Liu S, Zhou H, Qu LH, Yang JH (2014) StarBase v2.0: decoding miRNA-ceRNA, miRNA-ncRNA and protein-RNA interaction networks from large-scale CLIP-Seq data. Nucleic Acids Res 42:D92–97. https://doi.org/10.1093/nar/gkt1248
25. Karagkouni D, Paraskevopoulou MD et al (2019) DIANA-LncBase v3: indexing experimentally supported MiRNA targets on non-coding transcripts. Nucleic Acids Res. https://doi.org/10.1093/nar/gkz1036
26. Huang HY, Lin YC et al (2022) MiRTarBase update 2022: an informative resource for experimentally validated miRNA-target interactions. Nucleic Acids Res 50:D222–d230. https://doi.org/10.1093/nar/gkab1079
27. Shannon P, Markiel A et al (2003) Cytoscape: A software environment for integrated models of biomolecular interaction networks. Genome Res 13:2498–2504. https://doi.org/10.1101/gr.1239303
28. Krivoshein G, Tolner EA, Maagdenberg AVD, Giniatullin RA (2022) Migraine-relevant sex-dependent activation of mouse meningeal afferents by TRPM3 agonists. J Headache Pain 23:4. https://doi.org/10.1186/s10194-021-01383-8
29. Kukharsky MS, Ninkina NN et al (2020) Long non-coding RNA Neat1 regulates adaptive behavioural response to stress in mice. Translational Psychiatry 10:171. https://doi.org/10.1038/s41398-020-0854-2
30. An H, Tan JT, Shelkovnikova TA (2019) Stress granules regulate stress-induced paraspeckle assembly. J Cell Biol 218:4127–4140. https://doi.org/10.1083/jcb.201904098
31. Zhong F, Zhang W et al (2018) LncRNA NEAT1 promotes colorectal cancer cell proliferation and migration via regulating glial cell-derived neurotrophic factor by sponging miR-196a-5p. Acta Biochim Biophys Sin 50:1190–1199. https://doi.org/10.1093/abbs/gmy130
32. Her L-S, Mao S-H et al (2017) miR-196a enhances neuronal morphology through suppressing RANBP10 to provide neuroprotection in Huntington's disease. Theranostics 7:2452–2462. https://doi.org/10.7150/thno.18813
33. Miyazaki Y, Adachi H et al (2012) Viral delivery of miR-196a ameliorates the SBMA phenotype via the Silencing of CELF2. Nat Med 18:1136–1141. https://doi.org/10.1038/nm.2791
34. Chen Y, Mateski J et al (2024) Non-coding RNAs and neuroinflammation: implications for neurological disorders. Exp Biol Med 249:10120. https://doi.org/10.3389/ebm.2024.10120
35. Oberwinkler J, Philipp SE (2014) in Mammalian Transient Receptor Potential (TRP) Cation Channels: Volume I (eds Bernd Nilius & Veit Flockerzi), 427–459 Springer Berlin Heidelberg
36. Burglen L, Van Hoeymissen E et al (2023) Gain-of-function variants in the ion channel gene TRPM3 underlie a spectrum of neurodevelopmental disorders. eLife 12, e81032 https://doi.org/10.7554/eLife.81032
37. Grimm C, Kraft R, Sauerbruch S, Schultz G, Harteneck C (2003) Molecular and functional characterization of the Melastatin-related cation channel TRPM3*. J Biol Chemy 278:21493–21501. https://doi.org/10.1074/jbc.M300945200
38. Krivoshein G, Tolner EA, Maagdenberg A, Giniatullin RA (2022) Migraine-relevant sex-dependent activation of mouse meningeal afferents by TRPM3 agonists. J Headache Pain 23:4. https://doi.org/10.1186/s10194-021-01383-8

Publisher's note